

## PDF hosted at the Radboud Repository of the Radboud University Nijmegen

The following full text is a publisher's version.

For additional information about this publication click this link.

<http://hdl.handle.net/2066/84223>

Please be advised that this information was generated on 2017-12-06 and may be subject to change.

## Photoluminescence of PbS nanocrystals at high magnetic fields up to 30 T

L. Turyanska,<sup>1</sup> J. H. Blokland,<sup>2</sup> U. Elfurawi,<sup>1</sup> O. Makarovskiy,<sup>1</sup> P. C. M. Christianen,<sup>2</sup> and A. Patanè<sup>1,\*</sup>

<sup>1</sup>*School of Physics and Astronomy, The University of Nottingham, Nottingham NG7 2RD, United Kingdom*

<sup>2</sup>*High Field Magnet Laboratory, Institute for Molecules and Materials, Radboud University, Nijmegen 6525 ED, The Netherlands*

(Received 3 August 2010; revised manuscript received 13 October 2010; published 8 November 2010)

We use magnetic fields up to 30 T to study the circularly polarized magneto-photoluminescence (PL) of colloidal PbS nanocrystals. A semiclassical model for the population of polarized excitons is used to account for the measured magnetic field and temperature dependence of the degree of circular polarization of the PL emission and to probe the  $g$  factor,  $g_X$ , of the exciton. We report a systematic dependence of  $g_X$  on the nanocrystal size with values that increase from 0.1 to 0.3 at low temperature ( $T < 10$  K) with decreasing the nanocrystal diameter from 9 to 4 nm.

DOI: [10.1103/PhysRevB.82.193302](https://doi.org/10.1103/PhysRevB.82.193302)

PACS number(s): 73.21.La, 78.67.Hc, 78.55.-m, 71.35.Ji

The PbS and other lead chalcogenides (PbSe and PbTe) nanocrystals belong to a class of narrow energy gap (0.2–0.4 eV) IV-VI compounds with a unique electronic band structure and physical properties, which distinguish them from II-VI (CdSe, CdTe, etc.) and III-V (InAs, InP, etc.) quantum dots (QDs).<sup>1</sup> Beside the tunability of their energy spectrum in the near infrared region (NIR) and a regime of strong confinement of carriers, IV-VI QDs exhibit interesting excitonic phenomena, such as long recombination times ( $>100$  ns),<sup>2</sup> a complex exciton fine structure,<sup>3</sup> and an ultrafast fine-structure relaxation dynamics.<sup>4</sup> These properties result from the combination of bulk material properties, quantum confinement, electron-hole Coulomb and exchange interactions.<sup>3</sup> In particular, as the valence- and conduction-band originate both from the fourfold-degenerate  $L$  valleys of the Brillouin zone, the lead chalcogenides define an interesting type of excitonic prototype with the lowest-energy level corresponding to a nondegenerate dark state, followed at higher energy by a triple degenerate bright exciton state.<sup>3</sup>

In recent years, excitonic effects have been investigated in both self-assembled and colloidal quantum dots by magneto-optical studies.<sup>5–11</sup> Magneto-photoluminescence (PL) studies have provided useful means of probing the confinement and fine structure<sup>8</sup> of the exciton, as well as the dependence of the exciton  $g$  factor,  $g_X$ , on the lattice temperature,<sup>9</sup> electric field,<sup>10</sup> and on the size and shape of the QDs.<sup>11</sup> However, despite numerous studies of the physical properties of lead chalcogenide QDs and their exploitation in several applications,<sup>12–14</sup> their excitonic properties in magnetic field are still largely unexplored and are essential to test existing models of the electronic properties of these nanocrystals.

In this Brief Report, we use static magnetic fields,  $B$ , up to 30 T to investigate the circularly polarized magneto-PL of colloidal PbS nanocrystals with emission in the NIR (1000–1300 nm) and average diameter ranging from 4 to 9 nm. A semiclassical model for the population of polarized excitons is used to describe the magnetic field and temperature dependence of the degree of circular polarization (DCP) of the QD PL emission. In turn, this allows us to probe the  $g$  factor of the exciton and its dependence on the QD size.

For our studies we use colloidal thiol-capped PbS QDs synthesized in aqueous solution following the method pioneered by Levina *et al.*<sup>15</sup> These dots have approximately

spherical shape and diameter  $d$  tuneable in the range 4–9 nm depending on the molar ratio of the  $\text{Pb}^{2+}/\text{S}^{2-}$  reactants used to form the nanoparticles.<sup>16</sup> Solutions containing the QDs were stored under nitrogen atmosphere at  $T=5$  °C and were stable with respect to the morphological and PL properties over a period of at least 3 months. The magneto-PL study was performed under nonresonant excitation conditions on PbS QDs drop casted on a glass substrate. The optical excitation was provided by the 532 nm line of a solid-state laser ( $P=5 \times 10^4$  W/m<sup>2</sup>). The luminescence was dispersed by a 150 g/mm grating and detected by a nitrogen cooled (InGa)As array photodiode. The samples were mounted on an optical probe and cooled inside a liquid-helium bath cryostat in a 33 T Bitter-type electromagnet. Two circular polarizations,  $\sigma+$  and  $\sigma-$ , of the QD PL emission were measured in Faraday configuration using a circular polarizer at two successive sweeps of magnetic field with opposite directions. This study was performed with  $B$  up to 30 T in the temperature range 4.2–120 K.

Figure 1 shows the low-temperature ( $T=4.2$  K) unpolarized PL spectra of two ensembles of PbS QDs with average diameter  $d=5$  and 9 nm under applied magnetic fields  $B=0$  and 30 T. The magnetic field has two main effects on the QD PL spectrum; it redshifts the PL emission by  $\sim 1$  meV and decreases its intensity by  $\sim 5\%$ . At first sight, these effects are counterintuitive. In fact, an energy blueshift and an increase in intensity of the QD PL emission would be expected due to the extra confinement exerted by the magnetic field on the carriers. The diamagnetic shift,  $\delta E$ , depends on the size and shape of the exciton wave function according to the relation,  $\delta E = e^2 \langle \rho^2 \rangle B^2 / 8\mu_X$ , where  $\mu_X$  is the exciton reduced mass and  $\langle \rho^2 \rangle$  is the expectation value of the square of the electron-hole distance in the plane perpendicular to  $B$ .<sup>5</sup> To a first approximation  $\sqrt{\langle \rho^2 \rangle}$  is generally used as an estimate of the exciton size,  $\rho_X$ . For  $\rho_X \sim d/2$  and  $d$  in the range 4–9 nm, we estimate that  $2 < \delta E < 10$  meV at  $B=30$  T. Such energy shifts were not observed in any of the measured samples. This observation combined with the small redshift of the QD emission measured at high  $B$  suggests the existence of a competing physical mechanism counteracting the diamagnetic shift of the exciton states.

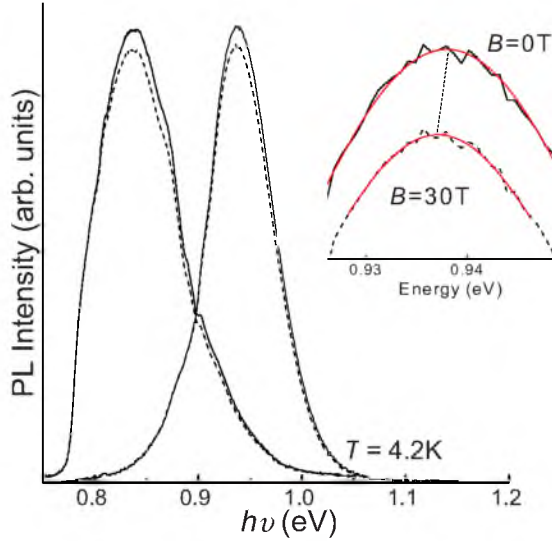


FIG. 1. (Color online) Low-temperature ( $T=4.2$  K) unpolarized PL spectra at  $B=0$  (continuous lines) and  $B=30$  T (dashed line) for PbS QDs with average diameter  $d=5$  and  $9$  nm. The inset shows the PL spectra around the peak for the sample with  $d=5$  nm and fits to the data by Gaussians.

To explore further the magnetic field dependence of the exciton states, we have studied the circular polarization properties of the QD PL emission. Figure 2(a) shows the low-temperature ( $T=7.5$  K) circularly polarized PL spectra at applied magnetic fields up to  $30$  T for QDs with average diameter  $d\sim 4$  nm. The DCP is calculated according to  $DCP=(I_{\sigma^-}-I_{\sigma^+})/(I_{\sigma^-}+I_{\sigma^+})$ , where  $I_{\sigma^+}$  and  $I_{\sigma^-}$  represent the peak intensities of the right and left circular polarized QD PL emission, respectively. As shown in Fig. 2(b), at low  $T$ , the DCP increases linearly with  $B$  at low fields ( $B<10$  T); a further increase in  $B$  leads to a sublinear increase in the DCP up to a value of  $\sim 30\%$  at  $B=30$  T. With increasing  $T$ , the DCP is significantly reduced. All our samples showed similar dependencies of the DCP on  $T$  and  $B$ . Figure 3(a) shows the  $B$  dependence of the low-temperature DCP for PbS QDs with different diameter. The value of the DCP at  $B=30$  T is in the range  $25\text{--}35\%$  and is comparable to that measured before for CdSe QDs (DCP  $>50\%$  at  $B=30$  T).<sup>6,7,9</sup> Differences among various colloidal nanocrystals can be caused by material properties and light scattering.

To provide a quantitative description of the DCP data, we use the semiclassical model of Ref. 17. The Zeeman interaction of the electron and hole spin with the magnetic field splits the degenerate bright exciton states with total angular momentum  $+1$  and  $-1$ . The lowest optically allowed bright excitons correspond to excitons with  $\text{spin}=\pm 1$  and Zeeman energy splitting given by  $\Delta E_{\theta}=g_X\mu_B B \cos \theta$ , where  $g_X$  is the exciton  $g$  factor,  $\mu_B$  is the Bohr magneton constant and  $\theta$  represents the angle between  $B$  and the preferential axis of polarization of the nanocrystal; since in these transitions electrons and holes have both  $s=1/2$  or  $s=-1/2$ , the exciton  $g$  factor can be also expressed as  $g_X=|g_e-g_h|$ . To account for the random orientation of the nanocrystals, the value of  $\theta$  is averaged out to generate the following expression for the DCP:<sup>18</sup>

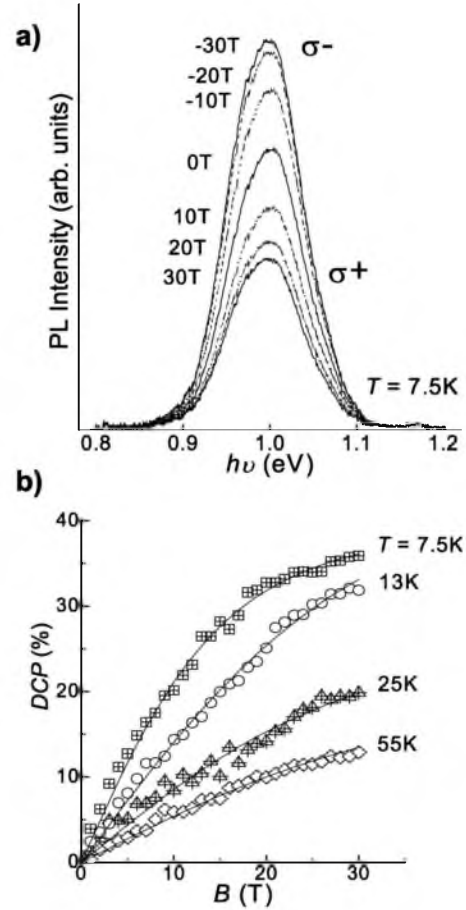


FIG. 2. (a) Circular-polarized PL emission at various magnetic fields for PbS QDs with average diameter  $d=4$  nm. (b)  $B$  dependence of the DCP of the QD PL emission at various temperatures for PbS QDs with  $d=4$  nm. Continuous lines are fit to the data by the model described in the text.

$$DCP = \frac{\int_0^{\pi} 2 \cos \theta \tanh(\Delta E/2k_B T) \sin \theta d\theta}{\int_0^{\pi} (1 + \cos^2 \theta) \sin \theta d\theta} \frac{1}{1 + \tau_s/\tau}. \quad (1)$$

Here  $\tau_s$  and  $\tau$  represent the spin relaxation and recombination time of the exciton, respectively. It can be seen from Eq. (1) that at low  $B$ , i.e.,  $\Delta E \ll k_B T$ , the DCP exhibits a linear dependence on  $B$  given by  $g_X \mu_B B / [4k_B T(1 + \tau_s/\tau)]$ . In contrast, in the limit of high  $B$ , i.e.,  $\Delta E \gg k_B T$ , the DCP exhibits only very small changes and approaches a constant value proportional to  $1/(1 + \tau_s/\tau)$ .

The calculated dependences of the DCP on  $B$  and  $T$  reproduce accurately the measured data. The DCP( $B$ ) curves at various  $T$  are shown in Fig. 2(b) for a QD sample with average diameter  $d=4$  nm. The calculated and measured low-temperature DCP( $B$ ) curves for QD samples with different  $d$  are shown in Fig. 3(a).

Let us first consider the QD sample with  $d=4$  nm (Fig. 2). At  $T=7.5$  and  $13.5$  K, the least-squares fit to the data by Eq. (1) is obtained with  $g_X=0.32 \pm 0.05$  and  $\tau_s/\tau=0.8 \pm 0.2$ ,

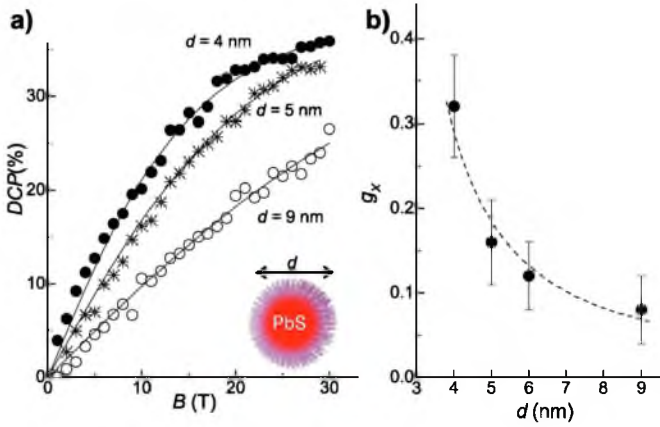


FIG. 3. (Color online) (a)  $B$  dependence of the DCP of the QD PL emission at low temperature for PbS QD samples with different values of  $d$ . Continuous lines are fit to the data by the model described in the main text. (b) Dependence of the exciton  $g$  factor on the average QD diameter  $d$  ( $T < 8$  K). The line is a guide to the eyes.

and  $g_X = 0.28 \pm 0.05$  and  $\tau_s/\tau = 0.6 \pm 0.2$ , respectively. At higher  $T$ , these parameters cannot be determined univocally due to the change in the form of the measured  $DCP(B)$  curve. We have also derived the  $DCP(B)$  curves by considering the PL intensity at different energies within the same QD PL band, see, for example, the  $DCP(B)$  curves of Fig. 4. For each curve, the measured data are reproduced accurately by the calculated dependence of the DCP on  $B$  with the same value of  $g_X$  (within the error bar) but slightly different values of  $\tau_s/\tau$ .

Our data and analysis for all our QD samples indicate a systematic increase in  $g_X$  with decreasing the average QD diameter. The value of  $g_X$  increases from  $g_X = 0.12 \pm 0.05$  for  $d = 9$  nm to  $g_X = 0.32 \pm 0.05$  for  $d = 4$  nm ( $T < 8$  K), see Fig. 3(b). An increase in  $g_X$  with decreasing the QD size was reported for InP nanocrystals;<sup>11</sup> also, measurements on self-assembled InGaAs/GaAs QDs have shown a high degree of tunability of  $g_X$  by varying the QD morphology<sup>11</sup> or by applying an external electric field.<sup>10</sup> These effects arise from quantum confinement and material properties<sup>9</sup> but were never reported before for PbS QDs. Also, since for bulk PbS it was shown that  $g_X \sim 0$ ,<sup>19</sup> we infer that the quantum confinement of carriers in PbS QDs has a strong effect on the  $g$  factor of the exciton.

These results are relevant to recent calculations of the excitonic exchange splitting and radiative lifetime of lead chalcogenides QDs, which have predicted a distinct type of excitonic exchange splitting pattern that is highly sensitive to the QD size.<sup>3</sup> Although our measurements on the QD ensemble do not reveal the exciton fine structure, the polarization data indicate a systematic dependence of the exciton polarization properties on the QD size, which has never been reported before for this type of nanocrystals. We also note that the values of  $g_X$  derived from the analysis of the DCP correspond to Zeeman energy splittings  $\Delta E$  less than 0.5

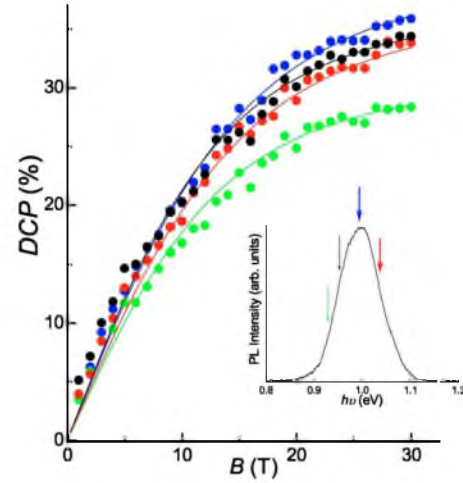


FIG. 4. (Color online)  $B$  dependence of the DCP at various energies for one of our PbS QD samples ( $T = 4.2$  K). Continuous lines are fit to the data by the model described in the text. Inset: QD PL spectrum with arrows showing the energy at which the DCP was measured.

meV at  $B = 30$  T. These energies are much smaller than the estimated diamagnetic shift of the QD PL emission at  $B = 30$  T ( $2 < \delta E < 10$  meV). Therefore we conclude that the Zeeman splitting of the bright exciton cannot be the only physical mechanism counteracting the diamagnetic shift of the QD PL emission. We propose that the admixing of the dark and bright exciton states at high  $B$  could provide a plausible explanation for the redshift and decrease in intensity of the QD PL emission observed at high  $B$  (Fig. 1). This phenomenon merits further investigation by optical spectroscopy of individual QDs and lifetime measurements to resolve the exciton fine structure and also to identify alternative recombination processes, i.e., phonon-assisted peaks, emission related to surface states, etc. Model calculations are also needed to describe the effect of a magnetic field on the exciton fine structure in PbS QDs and other IV-VI QDs, such as PbSe QDs, reported in the recent literature.<sup>20</sup>

In summary, PL experiments in magnetic fields up to 30 T were performed on ensembles of colloidal PbS nanocrystals with average size in the range 4–9 nm. In all samples, we have observed a large degree of circular polarization of the QD PL emission (DCP = 25–35% at  $B = 30$  T and  $T < 10$  K) and no diamagnetic energy shift. The data indicate a strong exciton confinement in the QD and the existence of a population of spin-polarized excitons. Also we find that, although the degree of PL polarization does depend on the QD size, the  $g$  factor of the exciton exhibits a systematic dependence on the nanocrystal size with values that range from 0.1 to 0.3 at low temperature.

This work is supported by the Leverhulme Trust, The University of Nottingham, and EuroMagNET II under the EU Contract No. 228043. We acknowledge useful discussions with N. R. Thomas.



\*Corresponding author: amalia.patane@nottingham.ac.uk

- <sup>1</sup>F. W. Wise, *Acc. Chem. Res.* **33**, 773 (2000).
- <sup>2</sup>H. Du, C. Chen, R. Krishnan, T. D. Krauss, J. M. Harbold, F. W. Wise, M. G. Thomas, and J. Silcox, *Nano Lett.* **2**, 1321 (2002).
- <sup>3</sup>J. M. An, A. Franceschetti, and A. Zunger, *Nano Lett.* **7**, 2129 (2007).
- <sup>4</sup>J. C. Johnson, K. A. Gerth, Q. Song, J. E. Murphy, and A. J. Nozik, *Nano Lett.* **8**, 1374 (2008).
- <sup>5</sup>For a review, see, for example, N. Miura, *Physics of Semiconductors in High Magnetic Fields* (Oxford University Press, New York, 2008).
- <sup>6</sup>M. Furis, J. A. Hollingsworth, V. I. Klimov, and S. A. Crooker, *J. Phys. Chem. B* **109**, 15332 (2005).
- <sup>7</sup>F. J. P. Wijnen, J. H. Blokland, P. T. K. Chin, P. C. M. Christianen, and J. C. Maan, *Phys. Rev. B* **78**, 235318 (2008).
- <sup>8</sup>L. Fradkin, L. Langof, E. Lifshitz, N. Gaponik, A. Rogach, A. Eychmüller, H. Weller, O. I. Micic, and A. J. Nozik, *Physica E* **26**, 9 (2005).
- <sup>9</sup>E. Johnston-Halperin, D. D. Awschalom, S. A. Crooker, A. L. Efros, M. Rosen, X. Peng, and A. P. Alivisatos, *Phys. Rev. B* **63**, 205309 (2001).
- <sup>10</sup>F. Klotz, V. Jovanov, J. Kierig, E. C. Clark, D. Rodolph, D. Heiss, M. Bichler, G. Abstreiter, M. S. Brandt, and J. J. Finley, *Appl. Phys. Lett.* **96**, 053113 (2010).
- <sup>11</sup>N. A. J. M. Kleemans, J. van Bree, M. Bozkurt, P. J. van Veldhoven, P. A. Nouwens, R. Nötzel, A. Yu. Silov, and P. M. Koeradi, *Phys. Rev. B* **79**, 045311 (2009).
- <sup>12</sup>B. R. Hyun, H. Chen, D. A. Rey, F. W. Wise, and C. A. Batt, *J. Phys. Chem. B* **111**, 5726 (2007).
- <sup>13</sup>A. L. Rogach, A. Eychmüller, S. G. Hickey, and S. V. Kershaw, *Small* **3**, 536 (2007).
- <sup>14</sup>S. A. McDonald, G. Konstantatos, S. Zhang, P. W. Cyr, E. J. D. Klem, L. Levina, and E. H. Sargent, *Nature Mater.* **4**, 138 (2005).
- <sup>15</sup>L. Levina, V. Sukhovatkin, S. Musikhin, S. Cauchi, R. Nisman, D. P. Bazett-Jones, and E. H. Sargent, *Adv. Mater.* **17**, 1854 (2005).
- <sup>16</sup>L. Turyanska, A. Patanè, M. Henini, B. Hennequin, and N. R. Thomas, *Appl. Phys. Lett.* **90**, 101913 (2007).
- <sup>17</sup>M. Chamarro, C. Gourdon, and P. Lavallard, *J. Lumin.* **70**, 222 (1996).
- <sup>18</sup>L. Langof, L. Fradkin, E. Ehrenfreund, E. Lifshitz, O. I. Micic, and A. J. Nozik, *Chem. Phys.* **297**, 93 (2004).
- <sup>19</sup>R. L. Bernick and L. Kleinman, *Solid State Commun.* **8**, 569 (1970).
- <sup>20</sup>R. D. Schaller, S. A. Crooker, D. A. Bussian, J. M. Pietryga, J. Joo, and V. I. Klimov, *Phys. Rev. Lett.* **105**, 067403 (2010).